$H_2O \underset{k_{1b}}{\overset{k_{1f}}{\rightleftarrows}} H^+ + OH^-$	k_{1f} = 10^8 s^{-1} k_{1b} = 10^{19} M^{-1} s^{-1}
$H_3PO_4 \underset{k_{2b}}{\overset{k_{2f}}{\rightleftarrows}} H_2PO_4^- + H^+$	k_{2f} = 10^7 s^{-1} k_{2b} = 1.32x10^9 M^{-1} s^{-1}
$H_2PO_4^- \underset{k_{3b}}{\overset{k_{3f}}{\rightleftarrows}} HPO_4^{2-} + H^+$	k_{3f} = 10^7 s^{-1} k_{3b} = 1.62x10^{14} M^{-1} s^{-1}
$HPO_4^{2-} \underset{k_{4b}}{\overset{k_{4f}}{\rightleftarrows}} PO_4^{3-} + H^+$	k_{4f} = 10^7 s^{-1} k_{4b} = 4.68x10^{19} M^{-1} s^{-1}
$CO_2 + H_2O \underset{k_{5f}}{\overset{k_{5b}}{\rightleftarrows}} H^+ + HCO_3^-$	k_{5f} = 0.036 s^{-1} k_{5b} = 7.83x10^4 M^{-1} s^{-1}
$CO_2 + OH^- \underset{k_{6b}}{\overset{k_{6f}}{\rightleftarrows}} HCO_3^-$	k_{6f} = 2.23x10^3 M^{-1} s^{-1} k_{6b} = 4.85x10^{-5} s^{-1}
$HCO_3^- \underset{k_{7b}}{\overset{k_{7f}}{\rightleftarrows}} H^+ + CO_3^{2-}$	k_{7f} = 2.5 s^{-1} k_{7b} = 5x10^{10} M^{-1} s^{-1}
$HCO_3^- + OH^- \underset{k_{8b}}{\overset{k_{8f}}{\rightleftarrows}} H_2O + CO_3^{2-}$	k_{8f} = 6x10^9 M^{-1} s^{-1} k_{8b} = 1.2 s^{-1}

Table S1 Forward and backward rate constants used in the modeling.

D_{H^+}	9.31 x 10^{-5} cm^2 s^{-1}	Diffusion coefficient of H^+
D_{OH^+}	5.26 x 10^{-5} cm^2 s^{-1}	Diffusion coefficient of OH^+
D_{CO}	1.02 x 10^{-5} cm^2 s^{-1}	Diffusion coefficient of CO
D_{CO_2}	1.92 x 10^{-5} cm^2 s^{-1}	Diffusion coefficient of CO_2
$D_{HCO_3^-}$	1.185 x 10^{-5} cm^2 s^{-1}	Diffusion coefficient of HCO_3^-
$D_{H_2PO_4^-}$	0.879 x 10^{-5} cm^2 s^{-1}	Diffusion coefficient of $H_2PO_4^-$
$D_{HPO_4^{2-}}$	0.439 x 10^{-5} cm^2 s^{-1}	Diffusion coefficient of HPO_4^{2-}
$D_{PO_4^{3-}}$	0.612 x 10^{-5} cm^2 s^{-1}	Diffusion coefficient of PO_4^{3-}
$D_{H_3PO_4}$	0.879 x 10^{-5} cm^2 s^{-1}	Diffusion coefficient of H_3PO_4
A	1 x 10^5 m^{-1}	Specific active surface area
α_e	0.35	transfer coefficient for C_2H_4 formation
α_m	1.33	transfer coefficient for CH_4 formation
α_{HER}	0.258	transfer coefficient for HER
J_e	1.18 x 10^{-8} mA cm^{-2}	Constant present in Eq (8) for C_2H_4 formation
J_m	3.47 x 10^{-18} mA cm^{-2}	Constant present in Eq (9) for CH_4 formation
i_{0_HER}	0.01 mA cm^{-2}	Exchange current density for HER

Table S2 Kinematic parameters used in the simulations.

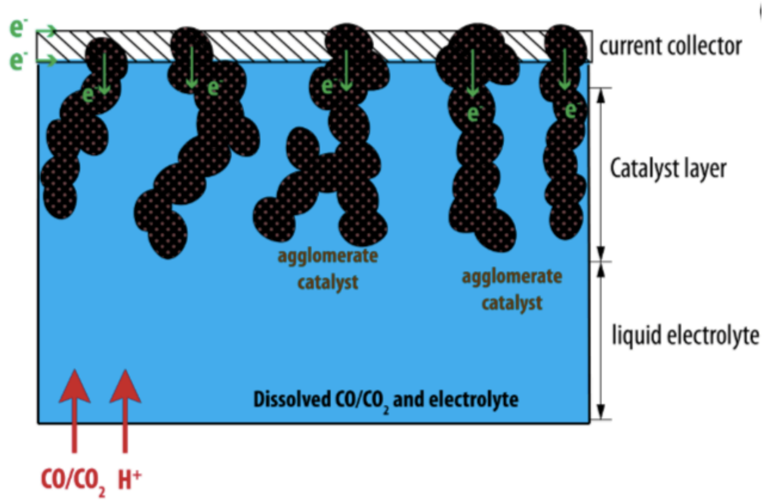

Figure S1 A schematic illustration of a nanostructured electrode

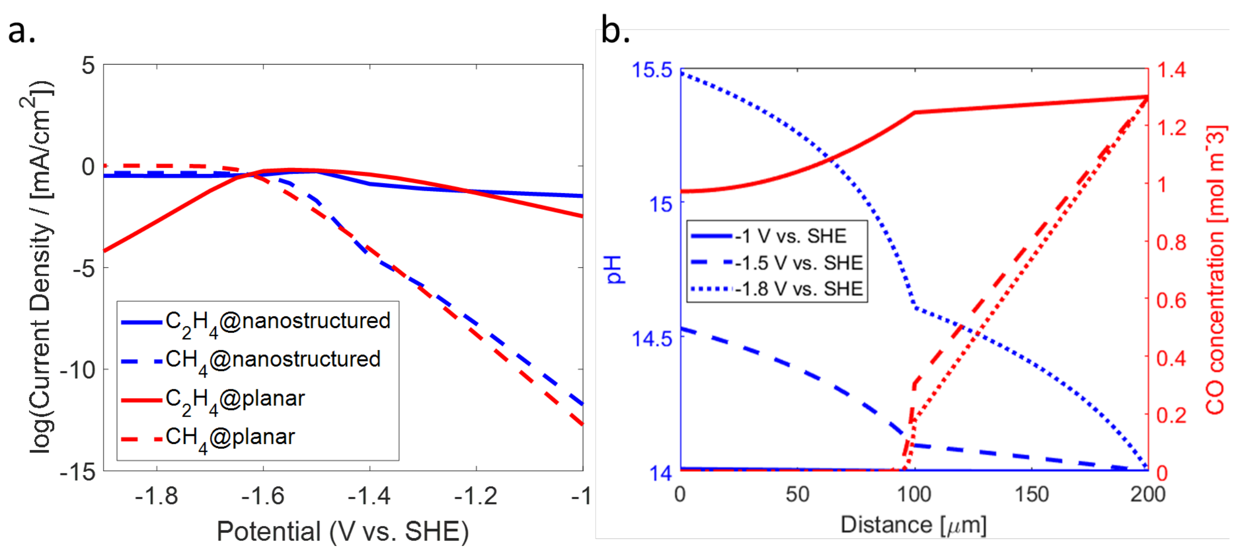

Figure S2 (a) The geometric partial current densities for CH_4 and C_2H_4 generation under the initial pH of 14 in both nanostructured- and planar electrode. (b) The spatially resolved pH and CO concentration for a nanostructured at different overpotentials

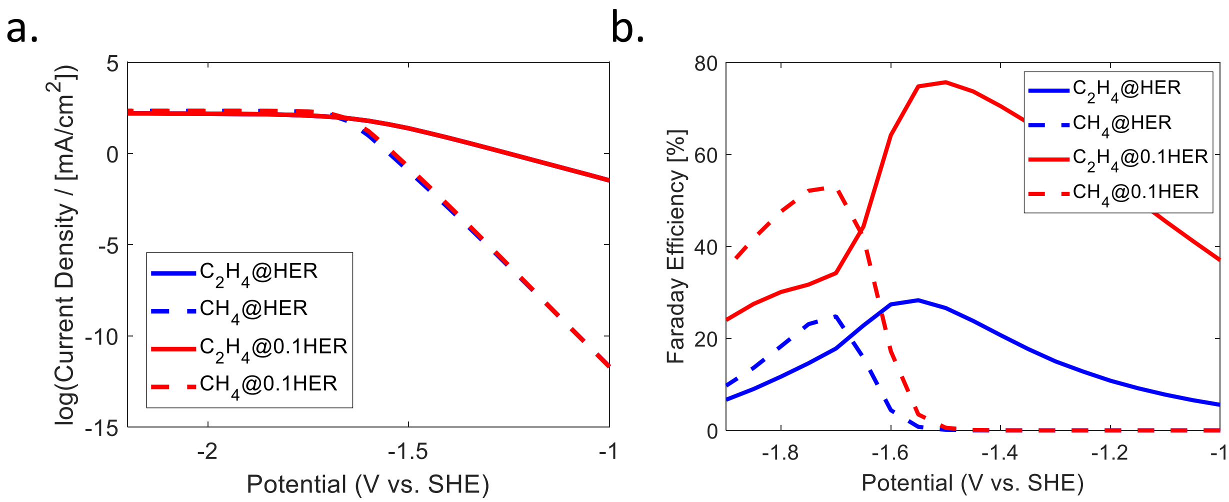

Figure S3 (a) The geometric partial current densities and (b) The Faraday efficiencies for CH_4 and C_2H_4 generation under different assumptions of CO coverage in the catalyst layer (@HER stands for low CO coverage and @0.1HER stands for high CO coverage)

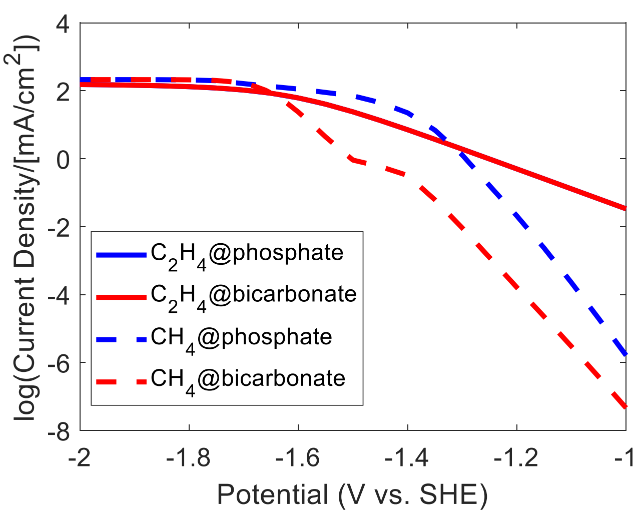

Figure S4 The geometric partial current densities for CH_4 and C_2H_4 generation with phosphate buffer and bicarbonate buffer, both under the initial pH value of 8.

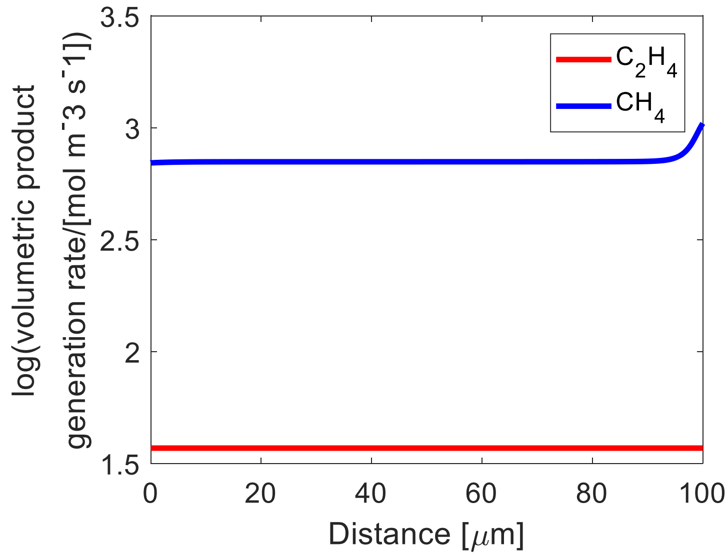

Figure S5 The volumetric product generation rates from CO_2 reduction as a function of position within GDE at -1.65 V vs. SHE.

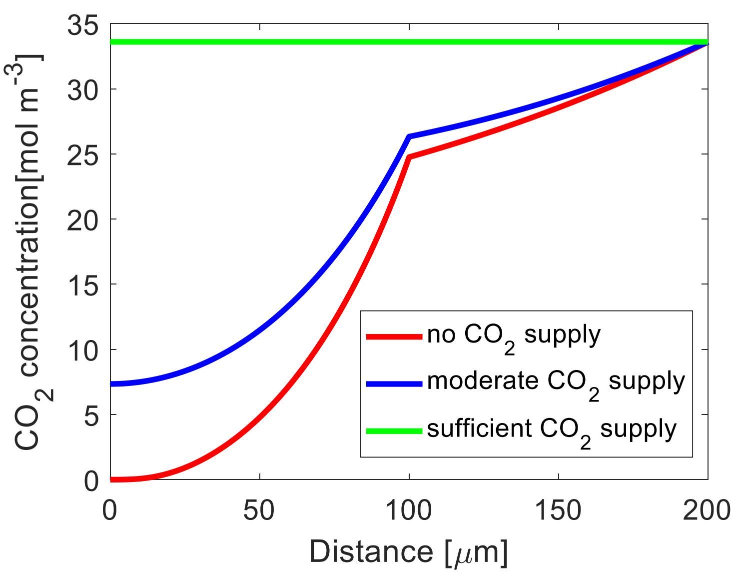

Figure S6 The CO_2 concentration as a function of position inside GDEs with different kinds of CO_2 supply at 1.4 V vs. SHE.

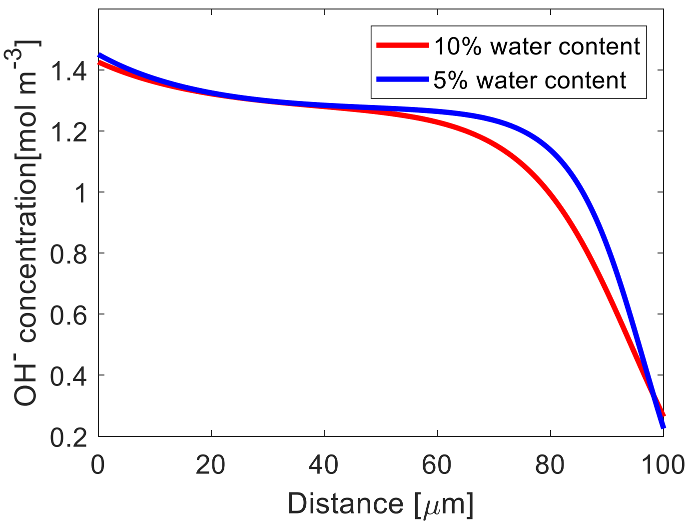

Figure S7 The OH^- concentration as a function of position inside GDEs with two different water content assumptions at -1.4 V vs. SHE.